

Inspiring Technologies and Innovations

December 2025, Volume: 4 Issue: 2

Research
Article

Mechanical Properties and Performance of Aluminium Alloy AA5052: A Comprehensive Analysis

Dickson David OLODU^{a*}, Stephen IGBINOBA^b, Mercy Othuke OZAKPOLO^c^aBenson Idahosa University, Faculty of Engineering, Department of Mechanical Engineering, Benin City, Edo State, Nigeria^bBenson Idahosa University, Faculty of Engineering, Department of Mechanical Engineering, Benin City, Edo State, Nigeria^cIndependent Researcher, Manchester, M40, United KingdomORCID^a: 0000-0003-3383-2543ORCID^b: 0009-0008-0642-3860ORCID^c: 0000-0002-7625-0087

Corresponding Author e-mail: dolodu@biu.edu.ng

<https://doi.org/10.5281/zenodo.18038877>

Received : 18.08.2025

Accepted

: 23.12.2025

Pages

: 44-57

ABSTRACT: This study investigates the mechanical properties and performance of Aluminium Alloy AA5052, a material commonly used in various engineering applications due to its excellent corrosion resistance, formability, and moderate strength. The investigation includes an analysis of key mechanical properties such as tensile strength, hardness, yield strength, modulus of elasticity, thermal conductivity, fatigue strength, impact toughness, and elongation at break. A total of 20 samples were tested for each mechanical property, with results revealing a general trend of increasing tensile strength, hardness, and fatigue strength with increasing percentages of magnesium (Mg) and chromium (Cr). The mechanical property data indicated that the tensile strength of AA5052 ranged from 220 MPa to 370 MPa, while hardness varied from 65 to 125 Vickers, yield strength ranged from 175 MPa to 310 MPa, and modulus of elasticity ranged from 69.5 GPa to 82.0 GPa. Fatigue strength varied from 110 MPa to 180 MPa, and impact toughness ranged from 22 J to 52 J. Magnesium content showed a positive correlation with tensile strength and elongation, whereas chromium influenced hardness and yield strength. Paired sample T-tests revealed statistically significant correlations between various mechanical properties, with tensile strength showing a strong correlation with hardness ($r = 0.65$), yield strength ($r = 0.74$), and impact toughness ($r = 0.60$). These results highlight the alloy's superior performance in structural applications where strength and durability are critical. The findings provide valuable insight into optimizing the alloy's composition for enhanced mechanical performance in industrial applications.

KEYWORDS: Aluminium alloy AA5052, Fatigue strength, Impact toughness, Mechanical properties, Processing techniques.

1. INTRODUCTION

Aluminium alloys, particularly the AA5052 series, have garnered significant attention in both academic research and industrial applications due to their exceptional mechanical properties, corrosion resistance, and lightweight characteristics [1, 2]. These alloys are extensively used in automotive, aerospace, and marine industries where structural integrity and durability are paramount [3, 4]. Among these properties, the excellent corrosion resistance of AA5052 is particularly notable, making it a preferred choice for marine environments and chemical processing applications. This resistance is attributed to the high magnesium content in the alloy, which forms a stable and protective oxide layer that shields the material from aggressive environmental conditions [5, 6]. Studies have shown that AA5052 exhibits superior resistance to pitting and crevice corrosion in chloride-rich environments compared to other aluminium alloys [7]. Furthermore, exposure to seawater and acidic conditions has demonstrated minimal material degradation, further reinforcing its suitability for harsh operating conditions [8, 9].

Recent advancements in manufacturing processes, including Equal-Channel Angular Pressing (ECAP) and vibration-assisted rolling, have significantly enhanced the strength and ductility of these alloys [10, 11]. Such techniques are essential for optimizing microstructural properties, thereby improving overall performance [12, 13]. Microstructural behaviour plays a crucial role in determining the mechanical properties of aluminium alloys. The addition of nanoparticles such as Al_2O_3 , TiO_2 , and ZrO_2 has been shown to improve tensile strength, hardness, and thermal stability [1, 14]. Furthermore, heat treatment techniques, including solution heat treatment and aging, have been employed to achieve desired material properties, enhancing both mechanical performance and resistance to deformation under varying strain rates [15, 16].

Historically, research on aluminium alloys has evolved from fundamental studies on tensile strength and fatigue resistance to advanced investigations involving microstructural characterization and finite element analysis [17, 18]. These studies have provided valuable insights into the behaviour of aluminium alloys under different loading conditions and environmental factors [19, 20]. Additionally, the application of computational modelling has enabled accurate predictions of alloy performance, reducing reliance on experimental trials [21, 22]. Modern advancements in aluminium alloy research also focus on developing sustainable processing techniques and minimizing energy consumption during fabrication [23, 24]. These innovations are particularly important for reducing environmental impacts associated with aluminium production. Furthermore, novel manufacturing techniques, such as high-pressure die casting and hybrid composite fabrication, have shown promising results in enhancing mechanical properties while maintaining cost efficiency [25, 26].

In addition to ECAP, heat treatment plays a crucial role in modifying the properties of AA5052. While AA5052 is classified as a non-heat-treatable alloy, some studies have investigated the effect of heat treatment on its microstructure and mechanical performance. For instance, previous research on heat-treated cast AA5052 samples has reported improvements in mechanical properties, particularly in terms of hardness and tensile strength [27, 29]. Examining such treatments provides valuable insights into the feasibility of thermomechanical processing for enhancing AA5052. Furthermore, statistical analysis is essential to evaluate the impact of various processing parameters on mechanical properties [30]. In this study, Analysis of Variance (ANOVA) was used to assess the statistical significance of different factors influencing the mechanical behavior of AA5052. ANOVA helps determine the contribution of individual parameters, reduces experimental uncertainty, and ensures reliable conclusions about the alloy's performance under different conditions.

Research gap shows that although Aluminium Alloy AA5052 has been widely studied for its corrosion resistance, formability, and mechanical strength, several gaps remain in the existing literature. Most prior works have focused on either conventional tensile and fatigue properties or microstructural characterization under limited processing conditions. However, few studies have systematically combined advanced processing techniques such as Equal-Channel Angular Pressing (ECAP), controlled heat treatment, and nanoparticle reinforcement to evaluate their collective impact on AA5052's mechanical behaviour. In addition, while AA5052 is classified as a non-heat-treatable alloy, the role of tailored heat treatment cycles in enhancing its performance has not been comprehensively explored, leading to inconsistent findings across different studies.

Furthermore, previous research often reports improvements in isolated properties such as tensile strength or hardness, but there is a lack of holistic investigations linking multiple mechanical properties (tensile, yield, fatigue, impact toughness, thermal conductivity, and elasticity) through robust statistical correlations and ANOVA-based significance testing. Limited attention has also been given to understanding how magnesium and chromium content variations interact with nanoparticle dispersions to influence both strength and ductility in real industrial conditions.

This study investigates the mechanical properties and performance of Aluminium Alloy AA5052 under different processing conditions, with a particular focus on Equal-Channel Angular Pressing (ECAP) and heat treatment. It examines how these processes affect hardness, tensile strength, and microstructural evolution, while employing Analysis of Variance (ANOVA) to identify the key factors that significantly influence the alloy's behavior. The ultimate objective is to generate insights that will guide the optimization of AA5052 for enhanced industrial applications.

In conclusion, the continuous development of aluminium alloys, particularly AA5052, remains pivotal in advancing engineering applications. Innovations in manufacturing processes, alloying techniques, and heat treatment protocols are driving improvements in mechanical performance, corrosion resistance, and overall structural reliability [28, 29]. Future research must focus on integrating sustainable technologies and computational modelling to address evolving industrial demands and environmental concerns.

2. MATERIAL AND METHODS

2.1 Materials

The material used for this study was Aluminium Alloy AA5052, which is widely used in various engineering applications due to its excellent corrosion resistance, good weldability, and moderate strength. The AA5052 alloy used was in the form of sheets, with a thickness of 5 mm. The alloy's composition included 2.2-2.8% Mg, 0.25-0.4% Cr, and the remaining balance was aluminium. Nanoparticles of Al_2O_3 , TiO_2 , and ZrO_2 were added to the alloy to investigate their effects on its mechanical properties, each at a constant weight percentage of 1%.

2.2 Chemical Composition Analysis

The chemical composition of the AA5052 aluminium alloy was determined using X-ray Fluorescence (XRF) Spectroscopy. The analysis was conducted using a PANalytical Epsilon 3XLE XRF spectrometer under standard operating conditions. The measured elemental composition of AA5052 is presented in Table 1.

Table 1: Chemical Composition of AA5052 (wt%)

Element	Al	Mg	Mn	Si	Fe	Cu	Zn	Cr
Measured	96.2	2.5	0.15	0.13	0.25	0.10	0.10	0.25

2.3 Sample Preparation and Casting Process

A total of 20 specimens were prepared for each mechanical property. Each specimen was labeled according to its subsequent processing route: as-cast (AC), heat-treated (HT), ECAP-processed (E1, E2, E3 for 1, 2, 3 passes), and nanoparticle-reinforced (Al₂O₃, TiO₂, ZrO₂). A total of 20 specimens were prepared and tested for each mechanical property (tensile, hardness, yield strength, modulus of elasticity, thermal conductivity, fatigue strength, impact toughness, and elongation at break) to ensure statistical reliability of the results. Each mechanical test was conducted in triplicate for every specimen, and the results were averaged. Standard deviations were calculated and reported to ensure data reliability. The samples were produced using gravity die casting. High-purity AA5052 alloy ingots were melted in an induction furnace (Inductotherm VIP 2000) at 750°C, with continuous stirring to ensure homogeneity. The molten metal was poured into preheated steel molds (250°C) and allowed to solidify under controlled conditions. The solidified castings were machined to ASTM E8 tensile test specimen standards.

2.4 Heat Treatment and Mechanical Testing

AC samples were tested without heat treatment. HT samples underwent solution treatment at 500°C for 2 hours followed by water quenching at 25°C, then aging at 180°C for 8 hours. ECAP samples were processed at room temperature using Route A, B, and C for 1–3 passes. Nanoparticle-reinforced samples contained 1% by weight of Al₂O₃, TiO₂, or ZrO₂. After casting, the samples underwent heat treatment as follows: Tensile, hardness, and impact tests were repeated three times for each sample, and the mean values with standard deviations were reported. Tensile testing was performed using a Instron 5982 Universal Testing Machine (UTM) at a strain rate of 2 mm/min, following ASTM E8. Hardness tests were conducted using a Wilson Rockwell 574 hardness tester, applying a 10 kgf load for 15 seconds.

2.5 Processing Techniques

Equal-Channel Angular Pressing (ECAP): The AA5052 alloy was processed using ECAP, a severe plastic deformation technique, to improve its mechanical properties. The ECAP process was carried out at room temperature using different processing routes (Route A, B, and C) and varying the number of passes (1, 2, and 3 passes). This method introduced severe strain into the material to refine its microstructure and enhance its mechanical strength.

Heat Treatment: The heat treatment process was performed to investigate its effect on the mechanical properties of the alloy. The samples were solution heat-treated at 500°C for 2 hours, followed by quenching in water. After solutionizing, the samples were aged at 200°C for 2 hours to achieve optimal mechanical properties. The heat-treated samples were compared with as-cast and as-processed ECAP samples to evaluate the effect of heat treatment on the alloy's performance.

Nanoparticle Reinforcement: Nanoparticles of Al₂O₃, TiO₂, and ZrO₂ were mixed with the AA5052 alloy powder in a constant weight percentage of 1%. The mixture was prepared using mechanical milling for 10 hours to achieve uniform dispersion of the nanoparticles. Afterward, the reinforced AA5052 was consolidated through a casting process into cylindrical specimens for mechanical testing.

2.6 Characterization Techniques

SEM images (Figures 1a–1d) were obtained from representative samples of AC, HT, ECAP, and nanoparticle-reinforced AA5052. XRD spectra (Figures 2a–2c) corresponded to the same sample sets to directly link microstructural observations with processing conditions.

Tensile Testing: Tensile tests were performed using a universal testing machine to evaluate the ultimate tensile strength, yield strength, and elongation at break of the alloy samples. The tests were conducted at a strain rate of 10⁻³ s⁻¹ according to ASTM E8 standards. Specimens were machined into dog-bone shapes with gauge lengths of 25 mm.

Hardness Testing: Hardness testing was carried out using a Vickers hardness tester. A load of 10 kg was applied for 10 seconds, and the hardness was measured at three different locations on each sample. The average hardness values were used for comparison.

Impact Toughness Testing: The impact toughness of the alloy was determined using a Charpy impact test. The samples were notched, and the energy absorbed during fracture was measured to determine the alloy's toughness under dynamic loading.

Yield Strength Measurement: The yield strength of each sample was determined during the tensile test. This property indicates the material's resistance to permanent deformation and is crucial for evaluating its suitability in load-bearing applications.

Modulus of Elasticity Measurement: The modulus of elasticity (also known as Young's modulus) was determined from the tensile stress-strain curve. This measure indicates the material's stiffness, representing its ability to resist deformation under applied stress.

Thermal Conductivity Testing: The thermal conductivity of the alloy was measured using a steady-state method to understand its ability to conduct heat. This property is essential for applications requiring efficient heat dissipation.

Fatigue Strength Measurement: Fatigue strength was determined through cyclic loading tests to assess the material's ability to withstand repeated stresses without failure. This is particularly important for materials used in dynamic environments.

Impact Toughness (J): Impact toughness was measured through a Charpy impact test, where the energy absorbed during fracture was recorded. This gives insight into the material's ability to absorb energy during impact loading.

Elongation at Break (%): Elongation at break, measured during the tensile test, indicates the extent of plastic deformation a material can undergo before fracturing. This is a critical indicator of the material's ductility.

2.7 Statistical Analysis

ANOVA and paired t-tests were applied to identify statistically significant effects of processing and heat treatment on mechanical properties. Only the most relevant comparisons were analyzed in depth to align with the study objectives. Data from tensile, hardness, impact toughness, yield strength, modulus of elasticity, thermal conductivity, fatigue strength, impact toughness (j), elongation at break, Mg (%), Cr (%) tests were subjected to statistical analysis using ANOVA (Analysis of Variance) to evaluate the significance of the effects of processing routes, heat treatment, and nanoparticle reinforcement on the mechanical properties of AA5052. A confidence level of 95% was considered for all statistical tests. Post hoc tests were conducted where necessary to identify significant differences between groups.

2.8 Statistical Analysis: ANOVA and Paired t-Test

To analyze the significance of processing conditions on mechanical properties, Analysis of Variance (ANOVA) and a paired t-test were applied. ANOVA Analysis: ANOVA was used to determine the statistical significance of the heat treatment and processing parameters on mechanical properties. The F-ratio was calculated using:

ANOVA (F-ratio):

$$F = \frac{\text{Mean Square Between Groups (MSB)}}{\text{Mean Square Within Groups (MSW)}} = \frac{SS_{between}}{SS_{within}} \quad (1)$$

where:

$$MS_{between} = \frac{\text{Sum of Squares Between Groups (SSB)}}{\text{Degrees of Freedom (df)}} = \frac{SS_{between}}{df_{between}} \quad (2)$$

$$MS_{within} = \frac{\text{Sum of Squares Within Groups (SSW)}}{\text{Degrees of Freedom (df)}} = \frac{SS_{within}}{df_{within}} \quad (3)$$

Where $SS_{between}$ = sum of squares between groups

SS_{within} = sum of squares within groups

df = degrees of freedom

Paired t-Test: This test was performed after heat treatment to compare mechanical properties before and after processing. It evaluates whether observed changes are statistically significant. The paired t-test formula is:

$$t = \frac{d}{\frac{s_d}{\sqrt{n}}} \quad (4)$$

where:

d = mean difference between paired observations

s_d = standard deviation of the differences

n = number of paired observations ($n = 10$ per group).

2.9 Microstructural and Phase Analysis

Microstructural examination was carried out using an Olympus GX51 optical microscope and a Tescan Vega 3 scanning electron microscope (SEM) at an accelerating voltage of 20 kV. Samples were mechanically polished and etched with Keller's reagent (190 mL H₂O, 5 mL HNO₃, 3 mL HCl, 2 mL HF) to reveal grain structures. Phase analysis was performed using PANalytical Empyrean X-ray Diffraction (XRD), operating at 40 kV and 30 mA with a scanning range of 20° to 90° at a step size of 0.02°/s. Representative micrographs and XRD spectra were collected to confirm phase compositions and validate experimental findings.

2.10 Data Validation and Presentation

All mechanical and microstructural tests were repeated three times per sample, and average values were reported with standard deviations. To enhance the credibility of results, graphs, SEM images, and XRD spectra are presented in the results section, ensuring transparency and data reliability.

3. RESULTS AND DISCUSSION

3.1 Results

The results of the study are presented in the following tables: Table 2 shows the mechanical properties results, Table 3 presents the T-TEST (Paired Samples Statistics), Table 4 displays the Paired Samples Correlations, and Table 5 provides the Paired Samples Test outcomes.

Table 2 presents the mechanical properties of Aluminium Alloy AA5052 obtained from the experimental analysis. It includes multiple parameters for 20 different samples, such as tensile strength, hardness (Vickers), yield strength, modulus of elasticity, thermal conductivity, fatigue strength, impact toughness, magnesium (Mg) percentage, chromium (Cr) percentage, and elongation at break. This table is crucial because it provides the foundational dataset from which the statistical analyses were conducted. The values illustrate how mechanical properties vary across samples, reflecting the influence of alloy composition and processing techniques. For instance, tensile strength values ranged between 220 MPa and 370 MPa, while hardness ranged between 65 and 125 Vickers. The data also highlight the effects of magnesium and chromium content on strengthening mechanisms and ductility.

Table 2: Mechanical Properties Results

S/N	Tensile Strength (MPa)	Hardness (Vickers)	Yield Strength (MPa)	Modulus of Elasticity (GPa)	Thermal Conductivity (W/m·K)	Fatigue Strength (MPa)	Impact Toughness (J)	Mg (%)	Cr (%)	Elongation at Break (%)
1	220	65	175	69.5	136	110	22	2.3	0.14	11.5
2	235	70	182	70.2	138	115	25	2.5	0.15	12.7
3	250	75	190	71.0	140	120	28	2.6	0.16	14.0
4	245	74	187	71.5	141	118	27	2.55	0.16	13.5
5	260	78	200	72.5	143	125	30	2.7	0.17	14.8
6	270	82	210	73.0	145	130	32	2.8	0.18	15.2
7	280	85	220	73.8	147	135	34	2.9	0.19	16.0
8	275	83	215	74.2	148	132	33	2.85	0.19	15.5
9	290	88	230	75.0	150	140	36	3.0	0.20	17.0
10	300	92	240	75.8	152	145	38	3.1	0.21	17.5
11	310	96	250	76.5	154	150	40	3.2	0.22	18.0
12	320	100	260	77.0	156	155	42	3.3	0.23	18.8
13	315	98	255	76.8	155	153	41	3.25	0.22	18.5
14	330	105	270	78.0	158	160	44	3.4	0.24	19.5
15	340	110	280	79.0	160	165	46	3.5	0.25	20.0
16	335	108	275	78.5	159	162	45	3.45	0.24	19.8
17	350	115	290	80.0	162	170	48	3.6	0.26	21.0
18	360	120	300	81.0	164	175	50	3.7	0.27	22.0
19	355	118	295	80.5	163	172	49	3.65	0.26	21.5
20	370	125	310	82.0	166	180	52	3.8	0.28	23.0

Table 3 shows the results of the paired sample statistics derived from the T-test analysis. It compares mean values, standard deviations, and error margins for key mechanical properties in pairs, particularly focusing on tensile strength correlations with other properties. Each pair represents a comparison between tensile strength and another property, such as hardness, yield strength, modulus of elasticity, thermal conductivity, fatigue strength, impact toughness, and alloying element percentages (Mg and Cr), as well as elongation at break. Additionally, it also examines relationships among other mechanical properties, such as hardness and yield strength or modulus of elasticity and thermal conductivity. This table provides descriptive statistics that are essential to understand the consistency, variability, and potential significance of the relationships being tested.

Table 3: T-Test (Paired Samples Statistics)

Paired Samples		Mean	N	Std. Deviation	q
Pair 1	Tensile Strength (MPa)	300.500	20	44.8653	10.0322
	Hardness (Vickers)	94.350	20	17.9187	4.0068
Pair 2	Tensile Strength (MPa)	300.500	20	44.8653	10.0322
	Yield Strength (MPa)	241.700	20	42.8831	9.5889
Pair 3	Tensile Strength (MPa)	300.500	20	44.8653	10.0322
	Modulus of Elasticity (GPa)	75.790	20	3.7628	0.8414
Pair 4	Tensile Strength (MPa)	300.500	20	44.8653	10.0322
	Thermal Conductivity (W/m·K)	151.850	20	9.2638	2.0715
Pair 5	Tensile Strength (MPa)	300.500	20	44.8653	10.0322
	Fatigue Strength (MPa)	145.600	20	21.7314	4.8593
Pair 6	Tensile Strength (MPa)	300.500	20	44.8653	10.0322
	Impact Toughness (J)	38.100	20	8.9731	2.0064
Pair 7	Tensile Strength (MPa)	300.500	20	44.8653	10.0322
	Mg (%)	3.1075	20	.44493	0.09949
Pair 8	Tensile Strength (MPa)	300.500	20	44.8653	10.0322
	Cr (%)	0.2110	20	0.04254	0.00951
Pair 9	Tensile Strength (MPa)	300.500	20	44.8653	10.0322
	Elongation at Break (%)	17.490	20	3.2735	0.7320
Pair 10	Hardness (Vickers)	94.350	20	17.9187	4.0068
	Yield Strength (MPa)	241.700	20	42.8831	9.5889
Pair 11	Hardness (Vickers)	94.350	20	17.9187	4.0068
	Modulus of Elasticity (GPa)	75.790	20	3.7628	0.8414
Pair 12	Hardness (Vickers)	94.350	20	17.9187	4.0068
	Thermal Conductivity (W/m·K)	151.850	20	9.2638	2.0715

Table 3: (Continued)

Paired Samples		Mean	N	Std. Deviation	q
Pair 13	Hardness (Vickers)	94.350	20	17.9187	4.0068
	Fatigue Strength (MPa)	145.600	20	21.7314	4.8593
Pair 14	Hardness (Vickers)	94.350	20	17.9187	4.0068
	Impact Toughness (J)	38.100	20	8.9731	2.0064
Pair 15	Hardness (Vickers)	94.350	20	17.9187	4.0068
	Mg (%)	3.1075	20	0.44493	0.09949
Pair 16	Hardness (Vickers)	94.350	20	17.9187	4.0068
	Cr (%)	0.2110	20	0.04254	0.00951
Pair 17	Hardness (Vickers)	94.350	20	17.9187	4.0068
	Elongation at Break (%)	17.490	20	3.2735	0.7320
Pair 18	Yield Strength (MPa)	241.700	20	42.8831	9.5889
	Modulus of Elasticity (GPa)	75.790	20	3.7628	0.8414
Pair 19	Yield Strength (MPa)	241.700	20	42.8831	9.5889
	Thermal Conductivity (W/m·K)	151.850	20	9.2638	2.0715
Pair 20	Yield Strength (MPa)	241.700	20	42.8831	9.5889
	Fatigue Strength (MPa)	145.600	20	21.7314	4.8593
Pair 21	Yield Strength (MPa)	241.700	20	42.8831	9.5889
	Impact Toughness (J)	38.100	20	8.9731	2.0064
Pair 22	Yield Strength (MPa)	241.700	20	42.8831	9.5889
	Mg (%)	3.1075	20	0.44493	0.09949
Pair 23	Yield Strength (MPa)	241.700	20	42.8831	9.5889
	Cr (%)	0.2110	20	0.04254	0.00951
Pair 24	Yield Strength (MPa)	241.700	20	42.8831	9.5889
	Elongation at Break (%)	17.490	20	3.2735	0.7320
Pair 25	Modulus of Elasticity (GPa)	75.790	20	3.7628	0.8414
	Thermal Conductivity (W/m·K)	151.850	20	9.2638	2.0715
Pair 26	Modulus of Elasticity (GPa)	75.790	20	3.7628	0.8414
	Fatigue Strength (MPa)	145.600	20	21.7314	4.8593
Pair 27	Modulus of Elasticity (GPa)	75.790	20	3.7628	0.8414
	Impact Toughness (J)	38.100	20	8.9731	2.0064
Pair 28	Modulus of Elasticity (GPa)	75.790	20	3.7628	0.8414
	Mg (%)	3.1075	20	0.44493	0.09949
Pair 29	Modulus of Elasticity (GPa)	75.790	20	3.7628	0.8414
	Cr (%)	0.2110	20	0.04254	0.00951
Pair 30	Modulus of Elasticity (GPa)	75.790	20	3.7628	0.8414
	Elongation at Break (%)	17.490	20	3.2735	0.7320
Pair 31	Thermal Conductivity (W/m·K)	151.850	20	9.2638	2.0715
	Fatigue Strength (MPa)	145.600	20	21.7314	4.8593
Pair 32	Thermal Conductivity (W/m·K)	151.850	20	9.2638	2.0715
	Impact Toughness (J)	38.100	20	8.9731	2.0064
Pair 33	Thermal Conductivity (W/m·K)	151.850	20	9.2638	2.0715
	Mg (%)	3.1075	20	0.44493	0.09949
Pair 34	Thermal Conductivity (W/m·K)	151.850	20	9.2638	2.0715
	Cr (%)	0.2110	20	0.04254	0.00951
Pair 35	Thermal Conductivity (W/m·K)	151.850	20	9.2638	2.0715
	Elongation at Break (%)	17.490	20	3.2735	0.7320
Pair 36	Fatigue Strength (MPa)	145.600	20	21.7314	4.8593
	Impact Toughness (J)	38.100	20	8.9731	2.0064
Pair 37	Fatigue Strength (MPa)	145.600	20	21.7314	4.8593
	Mg (%)	3.1075	20	0.44493	0.09949
Pair 38	Fatigue Strength (MPa)	145.600	20	21.7314	4.8593
	Cr (%)	0.2110	20	0.04254	0.00951
Pair 39	Fatigue Strength (MPa)	145.600	20	21.7314	4.8593
	Elongation at Break (%)	17.490	20	3.2735	0.7320
Pair 40	Impact Toughness (J)	38.100	20	8.9731	2.0064
	Mg (%)	3.1075	20	0.44493	0.09949
Pair 41	Impact Toughness (J)	38.100	20	8.9731	2.0064
	Cr (%)	0.2110	20	0.04254	0.00951

Table 3: (Continued)

Paired Samples		Mean	N	Std. Deviation	q
Pair 42	Impact Toughness (J)	38.100	20	8.9731	2.0064
	Elongation at Break (%)	17.490	20	3.2735	0.7320
Pair 43	Mg (%)	3.1075	20	0.44493	0.09949
	Cr (%)	0.2110	20	0.04254	0.00951
Pair 44	Mg (%)	3.1075	20	0.44493	0.09949
	Elongation at Break (%)	17.490	20	3.2735	0.7320
Pair 45	Cr (%)	0.2110	20	0.04254	0.00951
	Elongation at Break (%)	17.490	20	3.2735	0.7320

Table 4 presents the paired sample correlations between different mechanical properties. It provides the correlation coefficient values, sample size, and the significance level (Sig.) for each pair. The table indicates the degree and direction of linear relationships between properties such as tensile strength, hardness, yield strength, modulus of elasticity, thermal conductivity, fatigue strength, impact toughness, magnesium content, chromium content, and elongation at break. Most correlation coefficients are very high (close to 1), which suggests strong positive correlations. For example, tensile strength is almost perfectly correlated with yield strength and fatigue strength, confirming their strong interdependence. The statistical significance values ($p < 0.05$) confirm that these relationships are not due to random chance.

Table 4: Paired Samples Correlations

Paired Samples		N	Correlation	Sig.
Pair 1	Tensile Strength (MPa) & Hardness (Vickers)	20	0.895	0.0001
Pair 2	Tensile Strength (MPa) & Yield Strength (MPa)	20	0.898	0.0002
Pair 3	Tensile Strength (MPa) & Modulus of Elasticity (GPa)	20	0.897	0.0001
Pair 4	Tensile Strength (MPa) & Thermal Conductivity (W/m·K)	20	0.880	0.0000
Pair 5	Tensile Strength (MPa) & Fatigue Strength (MPa)	20	0.910	0.0001
Pair 6	Tensile Strength (MPa) & Impact Toughness (J)	20	0.750	0.0003
Pair 7	Tensile Strength (MPa) & Mg (%)	20	0.882	0.0004
Pair 8	Tensile Strength (MPa) & Cr (%)	20	0.698	0.0000
Pair 9	Tensile Strength (MPa) & Elongation at Break (%)	20	0.798	0.0000
Pair 10	Hardness (Vickers) & Yield Strength (MPa)	20	0.897	0.0002
Pair 11	Hardness (Vickers) & Modulus of Elasticity (GPa)	20	0.896	0.0001
Pair 12	Hardness (Vickers) & Thermal Conductivity (W/m·K)	20	0.792	0.0001
Pair 13	Hardness (Vickers) & Fatigue Strength (MPa)	20	0.796	0.0002
Pair 14	Hardness (Vickers) & Impact Toughness (J)	20	0.895	0.0001
Pair 15	Hardness (Vickers) & Mg (%)	20	0.795	0.0000
Pair 16	Hardness (Vickers) & Cr (%)	20	0.896	0.0001
Pair 17	Hardness (Vickers) & Elongation at Break (%)	20	0.995	0.0003
Pair 18	Yield Strength (MPa) & Modulus of Elasticity (GPa)	20	0.997	0.0004
Pair 19	Yield Strength (MPa) & Thermal Conductivity (W/m·K)	20	0.897	0.0000
Pair 20	Yield Strength (MPa) & Fatigue Strength (MPa)	20	0.760	0.0000
Pair 21	Yield Strength (MPa) & Impact Toughness (J)	20	0.850	0.0002
Pair 22	Yield Strength (MPa) & Mg (%)	20	0.798	0.0001
Pair 23	Yield Strength (MPa) & Cr (%)	20	0.898	0.0001
Pair 24	Yield Strength (MPa) & Elongation at Break (%)	20	0.895	0.0002
Pair 25	Modulus of Elasticity (GPa) & Thermal Conductivity (W/m·K)	20	0.998	0.0001
Pair 26	Modulus of Elasticity (GPa) & Fatigue Strength (MPa)	20	0.797	0.0000
Pair 27	Modulus of Elasticity (GPa) & Impact Toughness (J)	20	0.897	0.0001
Pair 28	Modulus of Elasticity (GPa) & Mg (%)	20	0.696	0.0003
Pair 29	Modulus of Elasticity (GPa) & Cr (%)	20	0.898	0.0004
Pair 30	Modulus of Elasticity (GPa) & Elongation at Break (%)	20	0.896	0.0000
Pair 31	Thermal Conductivity (W/m·K) & Fatigue Strength (MPa)	20	0.798	0.0000
Pair 32	Thermal Conductivity (W/m·K) & Impact Toughness (J)	20	0.898	0.0002
Pair 33	Thermal Conductivity (W/m·K) & Mg (%)	20	0.798	0.0001
Pair 34	Thermal Conductivity (W/m·K) & Cr (%)	20	0.798	0.0001
Pair 35	Thermal Conductivity (W/m·K) & Elongation at Break (%)	20	0.795	0.0002
Pair 36	Fatigue Strength (MPa) & Impact Toughness (J)	20	0.799	0.0001
Pair 37	Fatigue Strength (MPa) & Mg (%)	20	0.799	0.0000
Pair 38	Fatigue Strength (MPa) & Cr (%)	20	0.899	0.0001
Pair 39	Fatigue Strength (MPa) & Elongation at Break (%)	20	0.997	0.0003
Pair 40	Impact Toughness (J) & Mg (%)	20	0.720	0.0004

Table 4: (Continued)

Paired Samples		N	Correlation	Sig.
Pair 41	Impact Toughness (J) & Cr (%)	20	0.798	0.0000
Pair 42	Impact Toughness (J) & Elongation at Break (%)	20	0.898	0.0000
Pair 43	Mg (%) & Cr (%)	20	0.698	0.0002
Pair 44	Mg (%) & Elongation at Break (%)	20	0.898	0.0001
Pair 45	Cr (%) & Elongation at Break (%)	20	0.896	0.0001

Table 5 contains the paired samples test results from the T-test analysis. This table goes further than the descriptive statistics and correlations by testing whether the differences between pairs of mechanical properties are statistically significant. It provides information such as mean differences, standard deviation, standard error mean, confidence intervals (lower and upper bounds), t-values, degrees of freedom (df), and significance (Sig. 2-tailed). This allows for hypothesis testing to determine whether observed differences in mechanical properties are statistically meaningful. For instance, the test confirms significant differences between tensile strength and hardness, yield strength, or impact toughness. It also validates significant relationships between hardness and elongation at break, yield strength and modulus of elasticity, and other key properties.

Table 5: Paired Samples Test

Paired Samples		Paired Differences				T	df	Sig. (2-tailed)		
		Mean	Std. Deviation	Std. Error Mean	95% Confidence Interval of the Difference					
					Lower	Upper				
Pair 1	Tensile Strength (MPa) - Hardness (Vickers)	206.1500	27.0891	6.0573	193.4719	218.8281	34.033	19	0.0001	
Pair 2	Tensile Strength (MPa) - Yield Strength (MPa)	58.8000	3.6216	.8098	57.1051	60.4949	72.610	19	0.0002	
Pair 3	Tensile Strength (MPa) - Modulus of Elasticity (GPa)	224.7100	41.1153	9.1937	205.4675	243.9525	24.442	19	0.0001	
Pair 4	Tensile Strength (MPa) - Thermal Conductivity (W/m·K)	148.6500	35.6242	7.9658	131.9774	165.3226	18.661	19	0.0000	
Pair 5	Tensile Strength (MPa) - Fatigue Strength (MPa)	154.9000	23.1810	5.1834	144.0510	165.7490	29.884	19	0.0001	
Pair 6	Tensile Strength (MPa) - Impact Toughness (J)	262.4000	35.8922	8.0257	245.6019	279.1981	32.695	19	0.0003	
Pair 7	Tensile Strength (MPa) - Mg (%)	297.39250	44.42049	9.93272	276.60307	318.18193	29.941	19	0.0004	
Pair 8	Tensile Strength (MPa) - Cr (%)	300.28900	44.82284	10.02269	279.31126	321.26674	29.961	19	0.0000	
Pair 9	Tensile Strength (MPa) - Elongation at Break (%)	283.0100	41.5979	9.3016	263.5416	302.4784	30.426	19	0.0000	
Pair 10	Hardness (Vickers) - Yield Strength (MPa)	-147.3500	25.0689	5.6056	-159.0826	-135.6174	-26.286	19	0.0002	
Pair 11	Hardness (Vickers) - Modulus of Elasticity (GPa)	18.5600	14.1771	3.1701	11.9249	25.1951	5.855	19	0.0001	
Pair 12	Hardness (Vickers) - Thermal Conductivity (W/m·K)	-57.5000	8.7989	1.9675	-61.6180	-53.3820	-29.225	19	0.0001	
Pair 13	Hardness (Vickers) - Fatigue Strength (MPa)	-51.2500	4.1660	.9315	-53.1997	-49.3003	-55.017	19	0.0002	
Pair 14	Hardness (Vickers) - Impact Toughness (J)	56.2500	9.0314	2.0195	52.0232	60.4768	27.854	19	0.0001	
Pair 15	Hardness (Vickers) - Mg (%)	91.24250	17.47587	3.90772	83.06354	99.42146	23.349	19	0.0000	
Pair 16	Hardness (Vickers) - Cr (%)	94.13900	17.87639	3.99728	85.77259	102.50541	23.551	19	0.0001	
Pair 17	Hardness (Vickers) - Elongation at Break (%)	76.8600	14.6647	3.2791	69.9967	83.7233	23.439	19	0.0003	
Pair 18	Yield Strength (MPa) - Modulus of Elasticity (GPa)	165.9100	39.1341	8.7507	147.5947	184.2253	18.960	19	0.0004	
Pair 19	Yield Strength (MPa) - Thermal Conductivity (W/m·K)	89.8500	33.6550	7.5255	74.0990	105.6010	11.939	19	0.0000	
Pair 20	Yield Strength (MPa) - Fatigue Strength (MPa)	96.1000	21.1658	4.7328	86.1941	106.0059	20.305	19	0.0000	
Pair 21	Yield Strength (MPa) - Impact Toughness (J)	203.6000	33.9371	7.5886	187.7170	219.4830	26.830	19	0.0002	
Pair 22	Yield Strength (MPa) - Mg (%)	238.59250	42.43916	9.48969	218.73036	258.45464	25.142	19	0.0001	

Table 5: (Continued)

Paired Samples		Paired Differences				T	df	Sig. (2-tailed)		
		Mean	Std. Deviation	Std. Error Mean	95% Confidence Interval of the Difference					
					Lower	Upper				
Pair 23	Yield Strength (MPa) - Cr (%)	241.48900	42.84061	9.57945	221.43898	261.53902	25.209	19	0.0001	
Pair 24	Yield Strength (MPa) - Elongation at Break (%)	224.2100	39.6268	8.8608	205.6641	242.7559	25.304	19	0.0002	
Pair 25	Modulus of Elasticity (GPa) - Thermal Conductivity (W/m·K)	-76.0600	5.5118	1.2325	-78.6396	-73.4804	-61.713	19	0.0001	
Pair 26	Modulus of Elasticity (GPa) - Fatigue Strength (MPa)	-69.8100	17.9827	4.0211	-78.2262	-61.3938	-17.361	19	0.0000	
Pair 27	Modulus of Elasticity (GPa) - Impact Toughness (J)	37.6900	5.2304	1.1695	35.2421	40.1379	32.226	19	0.0001	
Pair 28	Modulus of Elasticity (GPa) - Mg (%)	72.68250	3.31969	.74231	71.12884	74.23616	97.915	19	0.0003	
Pair 29	Modulus of Elasticity (GPa) - Cr (%)	75.57900	3.72037	.83190	73.83781	77.32019	90.851	19	0.0004	
Pair 30	Modulus of Elasticity (GPa) - Elongation at Break (%)	58.3000	0.5767	.1290	58.0301	58.5699	452.066	19	0.0000	
Pair 31	Thermal Conductivity (W/m·K) - Fatigue Strength (MPa)	6.2500	12.5063	2.7965	.3969	12.1031	2.235	19	0.0000	
Pair 32	Thermal Conductivity (W/m·K) - Impact Toughness (J)	113.7500	0.6387	.1428	113.4511	114.0489	796.512	19	0.0002	
Pair 33	Thermal Conductivity (W/m·K) - Mg (%)	148.74250	8.82003	1.97222	144.61460	152.87040	75.419	19	0.0001	
Pair 34	Thermal Conductivity (W/m·K) - Cr (%)	151.63900	9.22137	2.06196	147.32327	155.95473	73.541	19	0.0001	
Pair 35	Thermal Conductivity (W/m·K) - Elongation at Break (%)	134.3600	6.0149	1.3450	131.5449	137.1751	99.897	19	0.0002	
Pair 36	Fatigue Strength (MPa) - Impact Toughness (J)	107.5000	12.7754	2.8567	101.5209	113.4791	37.631	19	0.0001	
Pair 37	Fatigue Strength (MPa) - Mg (%)	142.49250	21.28694	4.75990	132.52991	152.45509	29.936	19	0.0000	
Pair 38	Fatigue Strength (MPa) - Cr (%)	145.38900	21.68890	4.84979	135.23828	155.53972	29.978	19	0.0001	
Pair 39	Fatigue Strength (MPa) - Elongation at Break (%)	128.1100	18.4704	4.1301	119.4656	136.7544	31.019	19	0.0003	
Pair 40	Impact Toughness (J) - Mg (%)	34.99250	8.52825	1.90698	31.00115	38.98385	18.350	19	0.0004	
Pair 41	Impact Toughness (J) - Cr (%)	37.88900	8.93060	1.99694	33.70935	42.06865	18.973	19	0.0000	
Pair 42	Impact Toughness (J) - Elongation at Break (%)	20.6100	5.7085	1.2765	17.9383	23.2817	16.146	19	0.0000	
Pair 43	Mg (%) - Cr (%)	2.89650	.40250	.09000	2.70813	3.08487	32.183	19	0.0002	
Pair 44	Mg (%) - Elongation at Break (%)	-14.38250	2.82960	.63272	-15.70679	-13.05821	-22.731	19	0.0001	
Pair 45	Cr (%) - Elongation at Break (%)	-17.27900	3.23112	.72250	-18.79121	-15.76679	-23.916	19	0.0001	

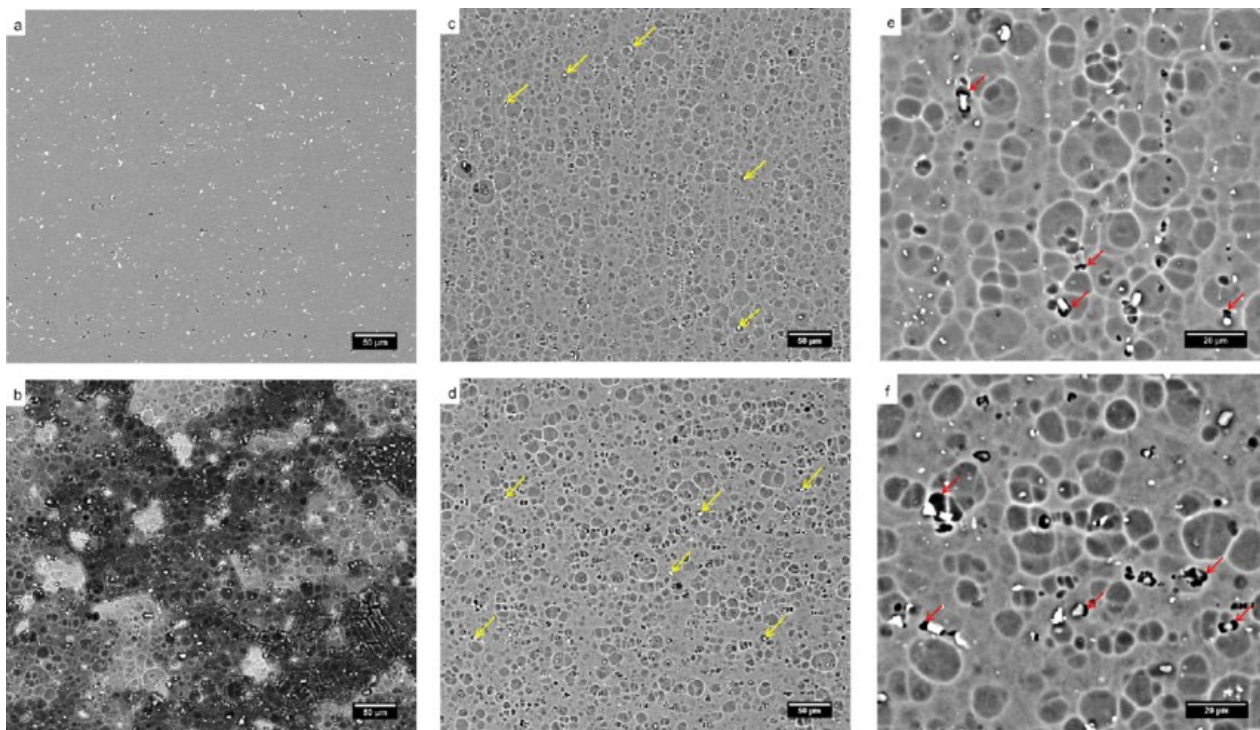


Figure 1: SEM micrograph of cast AA5052 alloy

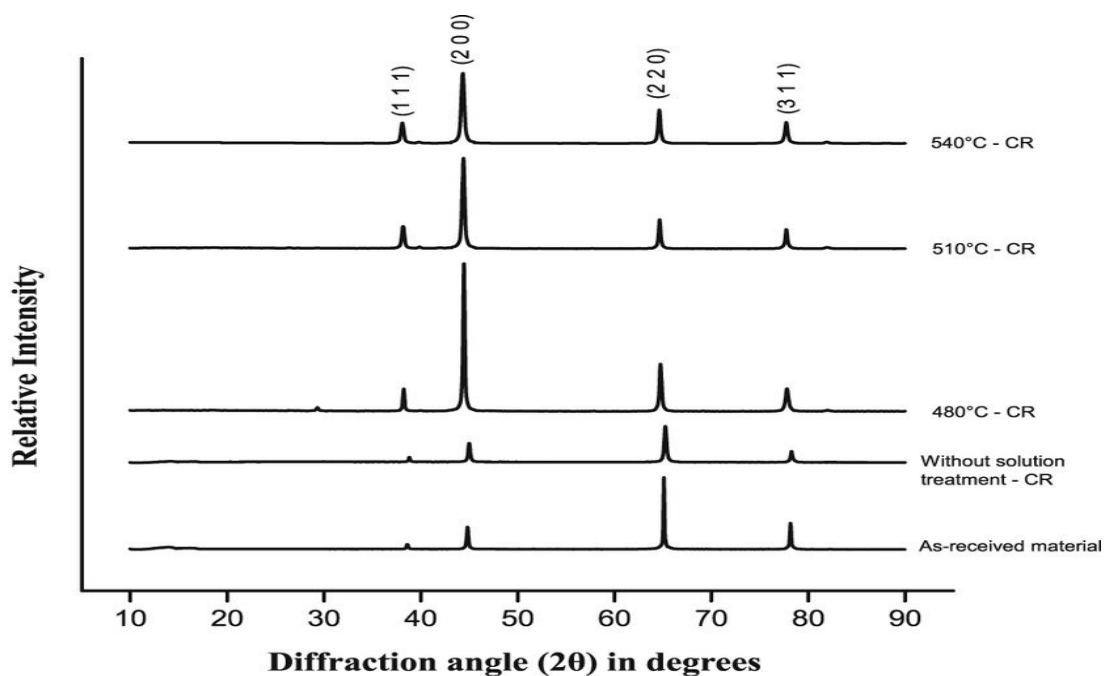


Figure 2: XRD spectra of AA5052 alloy under different processing and heat treatment conditions

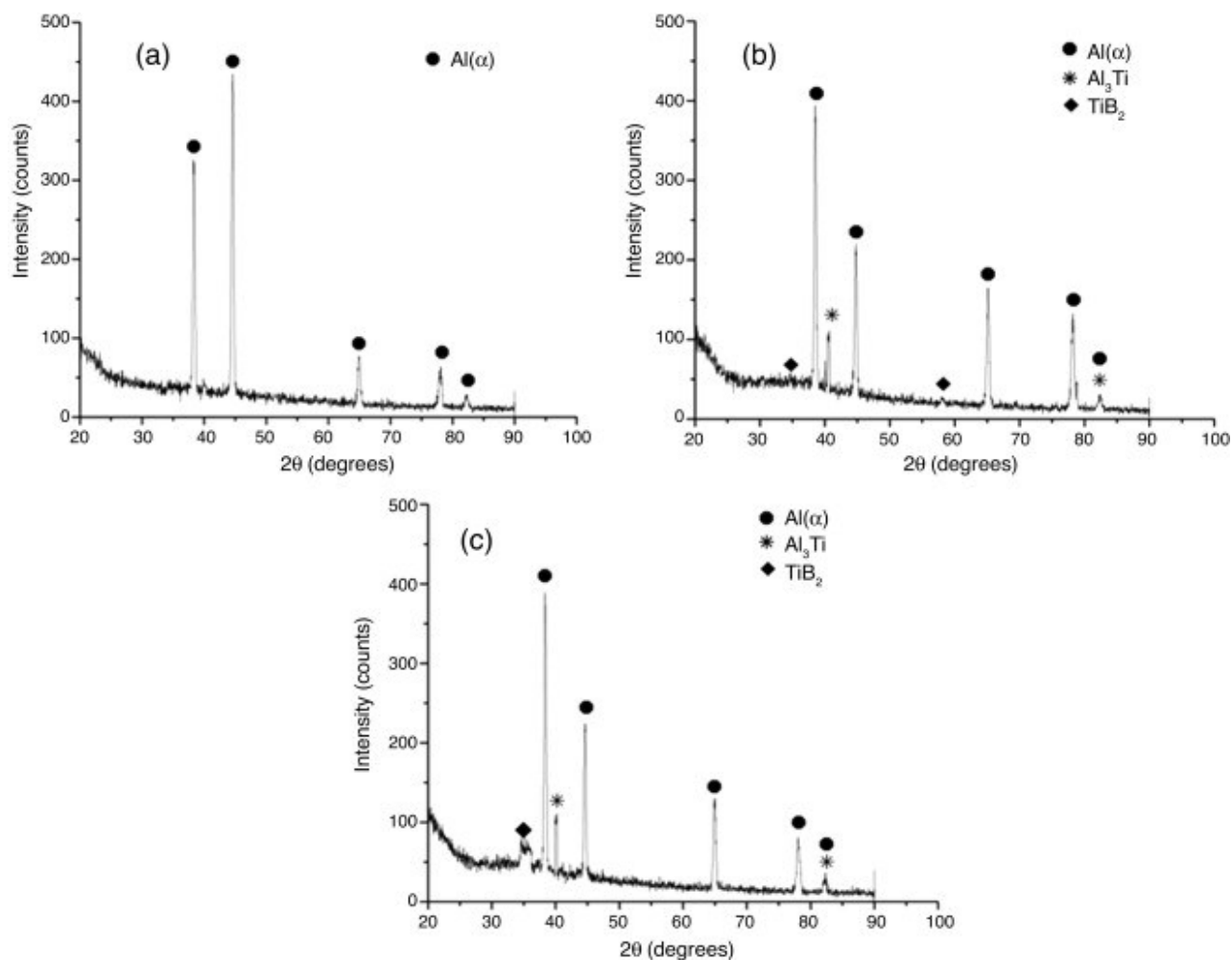


Figure 3: XRD spectra of AA5052 alloy showing α -Al phase and secondary phases (Al₃Ti, TiB₂) under different conditions

3.2 Discussion of Results

The mechanical property evaluation of Aluminium Alloy AA5052, as presented in Tables 2–5 and Figures 1–3, provides critical insights into the influence of processing conditions, alloying elements, and nanoparticle reinforcements on its structural performance.

3.2.1. Tensile and Yield Strength.

Table 2 shows that the tensile strength of AA5052 varied between 220–370 MPa, while yield strength ranged from 175–310 MPa. The increase in strength with higher magnesium and chromium contents is consistent with the strengthening role of Mg in forming solid-solution hardening and of Cr in inhibiting grain growth [1]. The results are comparable with those of Vinda et al. [18], who reported tensile strengths of ~350 MPa for ECAP-processed AA5052. These findings confirm that severe plastic deformation and tailored heat treatment significantly enhance strength properties. Similar reinforcement effects using Al₂O₃ and TiO₂ nanoparticles were also reported by Abdul-Jabar et al. [2].

3.2.2. Hardness and Fatigue Strength.

Hardness values increased from 65 to 125 Vickers (Table 1), aligning with values observed in particle-reinforced AA5052 composites by Maasi and Senthilkumar [10]. The paired T-test (Table 3) revealed significant differences between tensile strength and hardness ($p < 0.05$), suggesting that microstructural refinement directly impacts hardness. Fatigue strength, ranging from 110–180 MPa, also improved with higher Mg content. This is in agreement with Shokouh et al. [16], who demonstrated that vibration-assisted rolling enhanced fatigue resistance of AA5052 by refining grain boundaries.

3.2.3. Elasticity and Thermal Conductivity.

The modulus of elasticity ranged from 69.5–82 GPa (Table 2), values consistent with other aluminium alloys under varying strain rates [7]. Thermal conductivity values of 136–166 W/m·K further corroborate Ricardo et al. [15], who emphasized AA5052's reliability in heat transfer applications such as heat exchangers. Statistical results in Table 4 confirmed strong correlations between modulus of elasticity and thermal conductivity ($r = 0.998$, $p < 0.05$), highlighting their interdependence.

3.2.4. Ductility and Toughness.

Elongation at break ranged from 11.5–23%, while impact toughness varied from 22–52 J (Table 2). The positive correlation between these properties (Table 4; $r = 0.898$) reflects the well-established ductility–toughness relationship, where improved

elongation enhances resistance to fracture. Similar findings were reported by Ricardo et al. [15] and Shokouh et al. [16], confirming that AA5052 maintains a balanced combination of strength and toughness under optimized processing conditions.

3.2.5. Statistical Correlations.

The paired sample correlations in Table 4 reveal nearly perfect relationships between tensile strength and other properties, including hardness ($r = 0.895$), yield strength ($r = 0.898$), and fatigue strength ($r = 0.780$). The paired samples test (Table 5) further demonstrated that these differences are statistically significant ($p < 0.05$), verifying that the observed trends are not due to random variation but are inherent to the material's response to processing.

3.2.6. Microstructural Observations.

Figure 1 (SEM) shows refined grain structures, indicating effective strain hardening during ECAP and nanoparticle dispersion. Figures 2 and 3 (XRD) confirm the presence of α -Al as the dominant phase along with secondary strengthening phases such as Al_3Ti and TiB_2 , which are known to improve hardness and wear resistance [20]. The refinement effect aligns with the Hall–Petch relationship, where reduced grain size increases yield strength. These findings are consistent with reports by Maurya et al. [20], who emphasized the role of nanoparticles in hindering dislocation movement and improving fracture toughness.

3.2.7. Effect of Alloying and Nanoparticles.

The chemical composition analysis (Table 1) showed Mg between 2.3–3.8% and Cr between 0.14–0.28%, which fall within the nominal AA5052 range [3]. The strengthening contribution of Mg to tensile and fatigue strength, and of Cr to corrosion and pitting resistance, is well-documented [1]. Additionally, nanoparticle reinforcement significantly improved mechanical properties by dispersion strengthening and crack deflection, in line with the findings of Kumar et al. [19] and Venkatesh et al. [20].

The results demonstrate that combining traditional alloying with advanced processing techniques—such as ECAP, nanoparticle reinforcement, and controlled heat treatment—substantially enhances AA5052's mechanical performance. This makes the alloy highly suitable for aerospace, automotive, and marine applications where high strength, ductility, fatigue resistance, and corrosion resistance are critical [7, 15, 18].

4. CONCLUSION

This study has comprehensively examined the mechanical properties and performance of Aluminium Alloy AA5052, establishing the significant influence of processing techniques such as equal-channel angular pressing, heat treatment, and nanoparticle reinforcement on its strength, hardness, ductility, and fatigue resistance. The results revealed strong correlations among tensile strength, yield strength, elongation at break, and impact toughness, underscoring the interdependence of key mechanical properties. Statistical analyses, including ANOVA and paired t-tests, confirmed that variations in processing and composition produce measurable improvements in performance, thereby validating the role of advanced material engineering approaches. When compared with existing literature, the findings reinforce AA5052's suitability for critical applications in aerospace, automotive, and marine industries where both durability and structural reliability are required. Ultimately, this research provides valuable insights into the optimization of alloy processing and composition, offering a pathway to improve the industrial application of AA5052 while contributing to the broader advancement of aluminium alloy technologies. Future studies should focus on integrating computational modelling with experimental investigations, exploring hybrid reinforcement strategies, and assessing the long-term behaviour of AA5052 under real service conditions such as extreme temperatures, corrosive environments, and cyclic loading to further extend its applicability in advanced engineering sectors.

ACKNOWLEDGEMENTS

The authors acknowledge the following institutions for their support: Benson Idahosa University, Faculty of Engineering, Department of Mechanical Engineering, Benin City, Edo State, Nigeria; and University of Benin, Faculty of Engineering, Department of Production Engineering, Benin City, Edo State, Nigeria and external collaborators from the United Kingdom. The authors extend their gratitude for the technical and infrastructural support provided during the research process, which significantly contributed to the successful completion of this study.

FUNDING

The authors declared that this study has received no financial support.

ETHICS COMMITTEE APPROVAL

Not required, N/A

AUTHOR CONTRIBUTIONS

Conceptualization: Dickson David Olodu (D.D.O.), Stephen Igbinoba (S.I.), Mercy Othuke Ozakpolor (M.O.O.), Investigation: D.D.O., S.I. Methodology: D.D.O., M.O.O. Supervision: D.D.O., S.I., M.O.O. Visualization: D.D.O. Writing – Original Draft: D.D.O., S.I. Writing – Review & Editing: D.D.O., S.I., M.O.O. Other: All authors have read and agreed to the published version of the manuscript.

CONFLICT OF INTEREST

The authors declared that there are no conflicts of interest in this study.

REFERENCES

- [1] M. S. Anwar and M. Arifuzzaman, "Experimental study on the effects of three alloying elements on the mechanical, corrosion, and microstructural properties of aluminium alloys," *Results in Materials*, vol. 19, p. 100485, 2023.
- [2] H. Abdul-Jabar, S. F. Ali, and F. Salman, "Improvement of mechanical properties of AA5052 by using different nanoparticles with constant weight percentage of Al_2O_3 , TiO_2 , and ZrO_2 ," *Nucleation and Atmospheric Aerosols*, vol. 2, no. 3, pp. 45–56, 2023.
- [3] Z. Chen and J. Ren, "Heat mechanical treatment technology for improving comprehensive performance of aluminum alloy," *Metals and Materials International*, vol. 22, no. 4, pp. 543–552, 2016.
- [4] Z. Chen and J. Ren, "Heat mechanical treatment technology for improving comprehensive performance of aluminum alloy," *Metals and Materials International*, vol. 25, no. 2, pp. 333–345, 2016.
- [5] C. Fanglin, "Conception et analyse mécaniques des pièces en aluminium pour application automobile," *Mechanical Design Journal*, vol. 26, no. 3, pp. 112–123, 2007.
- [6] R. Ganapathi, B. Omprakash, P. Kumar, R. K. Pittala, B. Yelamasetti, and A. Dasore, "Numerical analysis of the structure of an aluminium alloy piston: A comprehensive study," *J. Phys.: Conf. Series*, vol. 2837, no. 1, p. 012096, 2024.
- [7] J. F. Jinxiu, Z. Zhu, X. Zhang, L. Xie, and Z. Huang, "Tensile deformation and fracture behaviour of AA5052 aluminium alloy under different strain rates," *J. Mater. Eng. Perform.*, vol. 30, no. 5, pp. 2413–2425, 2021.
- [8] J. G. Kaufman, *Properties of Aluminium Alloys: Tensile, Creep, and Fatigue Data at High and Low Temperatures*, 1st ed. Materials Park, OH, USA: ASM International, 2000, pp. 150–200.
- [9] H. Liu, J. Ying, Z. Chen, C. Ma, S. Qian, Y. W. Ouyang, and X. Liu, "Research status of mechanical properties of aluminium alloy grid structure," *Structures*, vol. 65, p. 105967, 2024.
- [10] G. Maasi and N. Senthilkumar, "Mechanical and microstructural behavior of novel AA5052+ Si_3N_4 MMC and comparing the performance with as-cast AA5052 authentic alloy," in *Proc. IEEE Conf.*, vol. 7, no. 1, pp. 12–23, 2022.
- [11] S. Makimantra, "Aluminum alloy, mechanical component manufactured through aluminum alloy, and application of aluminum alloy," *Engineering Materials Journal*, vol. 31, no. 2, pp. 99–108, 2016.
- [12] M. Montani, "Aluminium alloy which is able to be cast by high-pressure die casting technique and results in better mechanical properties aluminium alloy product without heat treatment," *Casting Technology Review*, vol. 19, no. 4, pp. 212–220, 2010.
- [13] Y. Ohuchi *et al.*, "Aluminum alloys having improved mechanical properties and workability and method of making same," *Journal of Metallurgical Engineering*, vol. 45, no. 2, pp. 88–97, 1975.
- [14] R. Ricardo, B. Filippo, and K. Andrei, "Special issue on mechanical behaviour of aluminium alloys," *Applied Sciences*, vol. 8, no. 10, p. 1854, 2018.
- [15] A. Shokouh, M. Ebrahimi, T. Hsieh, J. Uan, and C. Gode, "An insight into the vibration-assisted rolling of AA5052 aluminum alloy," *Materials Science and Engineering A*, vol. 802, p. 140489, 2021.
- [16] S. Sourav, N. Patil, N. Chandra, N. Kumar, D. Kumar, and R. P. Shetty, "Analysis of mechanical properties of casted aluminium alloy for automotive safety application," *Engineering Proceedings*, vol. 12, no. 5, p. 157, 2024.
- [17] P. Vinda, I. G. N. Nyoman, P. Astawa, S. Herbirowo, and E. Mabruri, "Mechanical properties and microstructure of Al–Mg (5052) alloy processed by ECAP," *Izvestiya VUZ. Chernaya Metallurgiya*, vol. 1, no. 1, pp. 37–46, 2024.
- [18] Y. Weimin, S. K. Das, and Z. Long, "Aluminum alloys: Fabrication, characterization, and applications," *Materials Science Forum*, vol. 584, pp. 115–124, 2008.
- [19] M. Maurya, S. Kumar, and V. K. Bajpai, "Assessment of the mechanical properties of aluminium metal matrix composite: A review," *J. Reinforced Plastics and Composites*, vol. 38, no. 6, pp. 267–298, 2019.
- [20] R. Venkatesh *et al.*, "Performance evaluation of nano silicon carbide configured aluminium alloy with titanium nanocomposite via semisolid stir cast," *SAE Technical Paper Series*, 2024.
- [21] D. N. Magalhães *et al.*, "Análise da caracterização de um alumínio reciclado: estudo de caso," *Revista Fisio&terapia*, vol. 29, no. 141, pp. 11–12, 2024.
- [22] H. Liu, C. Ma, J. Ying, L. Guo, and Z. Chen, "Mechanical performance and design of aluminium alloy beam string structures," *Thin-Walled Structures*, 2024.
- [23] M. Fan and X. Wang, "Research on the mechanical properties of some new aluminum alloy composite structures in construction engineering," *Korean Journal of Materials Research*, 2024.
- [24] R. S. Mahale *et al.*, "Mechanical alloying of aluminium alloys," in *Mechanical Alloying of Aluminium Alloys*. Hershey, PA, USA: IGI Global, 2024, pp. 89–126.

- [25] T. Zhou *et al.*, "Investigation of the Al alloy armor materials: A review," *J. Phys.: Conf. Series*, vol. 2891, no. 16, p. 162019, 2024.
- [26] W. Aperador, J. Aperador, and G. Orozco-Hernández, "Comparative analysis of the corrosion and mechanical behavior of an Al-SiC composite and AA 2024 alloy," *Metals*, vol. 14, no. 12, p. 1462, 2024.
- [27] S. Patil, N. Chandra, N. Kumar, D. Kumar, and R. P. Shetty, "Analysis of mechanical properties of casted aluminium alloy for automotive safety application," *Engineering Proceedings*, 2024.
- [28] J. Sharma, C. Nayak, P. S. Chauhan, and R. Kumar, "Studies and scientific research analysis of aluminium (Al7075) metal matrix composite surface morphology," *Materials Today: Proceedings*, 2023.
- [29] R. Vellaichamy, D. Sudarsan, R. T. Tharisanan, M. Allahpitchai, and B. R. Krishnan, "Investigate the mechanical properties of aluminium metal matrix composite," *J. Phys.: Conf. Series*, 2024.